Vol 16 No 11, November 2007
1009-1963/2007/16(11)/3339-06
Chinese Physics
© 2007 Chin. Phys. Soc.
and IOP Publishing Ltd

Differential cross sections of elastic electron scattering from CH_4, CF_4 and SF_6 in the energy range 100–700 eV*

Ma Er-Jun(马二俊)[a)b)c)], Ma Yu-Gang(马余刚)[a)], Cai Xiang-Zhou(蔡翔舟)[a)],
Fang De-Qing(方德清)[a)], Shen Wen-Qing(沈文庆)[a)], and Tian Wen-Dong(田文栋)[a)]

[a)] *Shanghai Institute of Applied Physics, Chinese Academy of Sciences, Shanghai* 201800, *China*
[b)] *Changshu Institute of Technology, Changshu* 215500, *China*
[c)] *Graduate School of Chinese Academy of Sciences, Beijing* 100039, *China*

(Received 31 January 2007; revised manuscript received 12 April 2007)

We investigate the differential cross sections (DCS) of elastic electron scattering from CH_4, CF_4 and SF_6 at six impact energies in a range of 100–700 eV by employing the independent atom model (IAM) together with the relativistic partial waves. The atom is present in an optical potential which is complex, spherically symmetric, and energy dependent. The optical potential of the atom is the sum of the direct static, dynamic polarization, local exchange and modified absorption potentials. The results obtained by using a modified absorption potential show significant improvements on the unmodified absorption potential results. The present results are generally in good agreement with experimental data available. In addition, the present results indicate that the structure of molecule manifests the observable effects on electron–molecule scattering.

Keywords: differential cross sections, independent atom model, electron–molecule scattering, relativistic partial waves, modified absorption potential

PACC: 3410, 3440, 3480

1. Introduction

Data of accurate differential cross sections (DCSs) for elastic electron scattering by molecules are required in a wide variety of research fields, such as gas lasers,[1] Monte Carlo simulations of electron transport,[2] plasma depositions, etching of semiconductor materials, gaseous high-voltage switches,[3] cell radiation damage[4] and interstellar/atmospheric process.[5] Theoretically a number of methods are developed to predict DCSs for elastic electron–molecule scattering. In the low-energy range there are R-matrix method,[6] close-coupling method,[7] the momentum-space-coupled channel optical method[8] and finite-element R-matrix method[9,10] that are complex and time consuming in computation. In the high-energy range the Born approximation, the Glauber approximation and the eikonal approximation[11] can give results that are generally in agreement with experimental data. However, almost all inelastic channels (rotational, vibrational, and electronic excitation, ionization processes, etc.) are open in the intermediate-energy region. Consequently the methods applicable for low-energy electron scattering from molecules are difficult and almost impossible to be directly applied in this energy region.

Some approximate methods have been developed to obtain cross sections of electron-molecule scattering at intermediate energies. Iga *et al*[12] applied the Schwinger variational iterative method combined with the distorted-wave approximation to calculating the scattering amplitudes. Jain and Baluja[13] proposed the spherical complex optical potential approach to the investigation of the total cross sections for electron scattering from a series of molecules. In addition, additivity rule (AR) model[14−20] and the independent atom model (IAM)[21,22] have been widely used to explore electron–molecule collisions. It is well known that absorption effects should be taken into account in the intermediate energy range. So all these methods utilize the model absorption potential for treating electron–molecule collisions in this energy range. Indeed, several model absorption potentials with both empirical[23−25] or nonempirical[26,27] nature for electron–atom scattering have been proposed for more than 20 years. Among these model poten-

*Project supported by the Shanghai Development Foundation from Science and Technology, China (Grant Nos 06JC14082 and 06QA14062), the National Natural Science Foundation of China (Grant No 10535010), and the Knowledge Innovation Project of Chinese Academy of Sciences (Grant No KJXC3-SYW-N2).

tials, the quasifree scattering model (QFSM) proposed by Staszewska *et al* has been widely used. The QFSM was derived non-empirically to reproduce the absorption probability per unit time for an electron passing through a free-electron gas, where the electron-electron absorption cross sections are calculated using the Pauli-allowed binary-encounter approximation. Khare *et al*[28] applied the IAM combined with the absorption potential of Staszewska *et al* to investigate the elastic electron scattering from CF_4 (carbon tetrafluoride) at energies ranging from 100 to 700 eV. Their results have indicated that, at large scattering angles, at first the theoretical DCSs lie above the measured data and then gradually appear under the measured data with increasing incident energies. This means that the absorption potential of Staszewska *et al*[27] overestimated the flux loss to the electronic excited states for large scattering angles, particularly at high incident energies. The same conclusion can be deduced from a number of investigations.[22,27,29] In view of analysis stated above, we empirically propose an energy-dependent factor (Eq.(12)) that is multiplied by the absorption potential of Staszewska *et al* to improve the degree of agreement between theory and experiment.

To check the validity of the present modification of the absorption potential of Staszewska *et al*, we choose CH_4 (methane), CF_4 (carbon tetrafluoride) and SF_6 (sulfur hexafluoride) to calculate the DCSs for electron scattering using the IAM because these molecules are all highly symmetric and are favourable for the use of the IAM. Although there has existed some literature[28,30,31] that is devoted to elastic electron scattering from these molecules by virtue of the IAM, to our knowledge there is no literature that investigates these molecules simultaneously. So we expect to expose the influence of the molecular structure on the elastic electron scattering in the present investigation.

2. Theory and method

In the IAM, electron–molecule collisions are reduced to electron interactions with individual atoms of the target molecule. This reduction is based on the following assumptions: (i) each atom of the molecule scatters independently; (ii) redistribution of atomic electrons due to molecular binding is unimportant; and (iii) multiple scatterings within the molecule are negligible.[32] According to the IAM, the scattered wave at large distances from the molecule is approximated as the coherent sum of the wave functions scattered from all atoms in the molecule. The DCSs averaged over all orientations of the molecular axis in the IAM is given by

$$I(\theta) = \sum_{i,j=1}^{N} \frac{\sin(q\, r_{ij})}{q\, r_{ij}} [f_i(\theta) f_j^*(\theta) + g_i(\theta) g_j^*(\theta)], \quad (1)$$

where $f_i(\theta)$ and $g_i(\theta)$ are the direct and spin-flip scattering amplitudes, respectively, for the ith atom in the molecule. r_{ij} and N are, respectively, the separation between the ith atom and the jth atom, and the total number of atoms present in the molecule. q is the magnitude of the momentum transfer in the collisions.

The direct and spin-flip scattering amplitudes admit the following partial waves expansions:[33]

$$f(\theta) = \frac{1}{2\mathrm{i}k} \sum_{\ell=0}^{\infty} \{(\ell+1)[\exp(2\mathrm{i}\delta_{\kappa=-\ell-1}) - 1] + \ell[\exp(2\mathrm{i}\delta_{\kappa=\ell}) - 1]\} P_\ell(\cos\theta), \quad (2)$$

and

$$g(\theta) = \frac{1}{2\mathrm{i}k} \sum_{\ell=0}^{\infty} [\exp(2\mathrm{i}\delta_{\kappa=\ell}) - \exp(2\mathrm{i}\delta_{\kappa=-\ell-1})] P_\ell^1(\cos\theta) \quad (3)$$

respectively, where k is the relativistic wavenumber of the electron. $P_\ell(\cos\theta)$ and $P_\ell^1(\cos\theta)$ are the Legendre polynomials and associated Legendre functions, respectively.

To obtain the values of phase shift δ_κ, the following coupled differential equations are solved numerically under the appropriate boundary conditions,

$$\begin{aligned} \frac{\mathrm{d}P_{E\kappa}(r)}{\mathrm{d}r} &= -\frac{\kappa}{r} P_{E\kappa}(r) + \frac{E - V_{\mathrm{opt}} + 2m_{\mathrm{e}}c^2}{c\hbar} Q_{E\kappa}(r), \\ \frac{\mathrm{d}Q_{E\kappa}(r)}{\mathrm{d}r} &= -\frac{E - V_{\mathrm{opt}}}{c\hbar} P_{E\kappa}(r) + \frac{\kappa}{r} Q_{E\kappa}(r), \end{aligned} \quad (4)$$

where κ is the relativistic quantum number. $P_{\mathrm{E}\kappa}(r)$ and $Q_{\mathrm{E}\kappa}(r)$ are the radial functions of the Dirac spherical waves. E is the kinetic energy of the incident electron and V_{opt} is the appropriate complex optical potential which incorporates all the important effects,

$$V_{\mathrm{opt}} = V_{\mathrm{s}}(r) + V_{\mathrm{p}}(r) + V_{\mathrm{ex}}(r) - \mathrm{i}V_{\mathrm{a}}'(r), \quad (5)$$

where $V_{\mathrm{s}}(r)$, $V_{\mathrm{p}}(r)$, $V_{\mathrm{ex}}(r)$, and $V_{\mathrm{a}}'(r)$ are the static, polarization, exchange, and absorption potentials, respectively for electron–atom interactions. For the electron density function $\rho(r)$, we employ the analytical expressions of Salvat,[34] obtained by a fit-

ting procedure to the Dirac–Hartree–Fock–Slater self-consistent data. It is given by

$$\rho(r) = \frac{Z}{4\pi r}\sum_{i=1}^{3} A_i\alpha_i^2 \mathrm{e}^{-\alpha_i r}, \tag{6}$$

where A_i and α_i are the parameters tabulated in Ref.[34]. If we neglect the finite extent of the nuclear charge distribution, by virtue of $\rho(r)$, the static potential $V_\mathrm{s}(r)$ can be expressed as

$$V_\mathrm{s}(r) = -\frac{Z}{r} + \int \frac{\rho(r')}{r_>}\mathrm{d}^3 r', \tag{7}$$

where Z is the nuclear charge and $r_>$ is the greater between r and r'. For $V_\mathrm{ex}(r)$, we use the exchange potential of Furness and McCarthy,[35] which is derived directly from the formal expression of the non-local exchange interaction by using the Wentzel–Kramers–Brillouin (WKB)-like approximation for the wave functions, and we obtain

$$\begin{aligned} V_\mathrm{ex}(r) = {} & \frac{1}{2}[E - V_\mathrm{s}(r)] \\ & -\frac{1}{2}\{[E - V_\mathrm{s}(r)]^2 + 4\pi a_0 \rho(r)\}^{1/2}, \end{aligned} \tag{8}$$

where a_0 is the Bohr radius. As for $V_\mathrm{p}(r)$, it is expressed by the Buckingham polarization potential[36]

$$V_\mathrm{p}(r) = -\frac{\alpha_\mathrm{p}}{2}\frac{1}{(r^2 + r_\mathrm{c}^2)^2}, \tag{9}$$

where α_p is the dipole polarizability of the target atom and r_c is the cut-off parameter[37] that serves to prevent the polarization potential from diverging at $r = 0$. For the absorption potential which models a loss of flux from the elastic channels to inelastic channels when the incident energy of electrons is above the first excitation threshold, it is given by

$$V_\mathrm{a}'(r) = mV_\mathrm{a}(r), \tag{10}$$

where $V_\mathrm{a}(r)$ is the absorption potential proposed by Staszewska *et al*[27]

$$V_\mathrm{a}(r) = \frac{8\pi\rho(T_\mathrm{L}/2)^{1/2}}{5k^2k_\mathrm{f}^3}H(x)(A + B), \tag{11}$$

with

$$\begin{aligned} A &= 5k_\mathrm{f}^3/(2\Delta) - k_\mathrm{f}^3(5k^2 - 3k_\mathrm{f}^2)/(k^2 - k_\mathrm{f}^2)^2, \\ B &= 2H(y)y^{5/2}/(k^2 - k_\mathrm{f}^2)^2, \\ x &= k^2 - k_\mathrm{f}^2 - 2\Delta, \\ y &= 2k_\mathrm{f}^2 + 2\Delta - k^2, \end{aligned}$$

where $k_\mathrm{f}(r) = [3\pi^2\rho(r)]^{1/3}$ is the local Fermi wavenumber of the atomic electron cloud; $T_\mathrm{L}(r) = E - V_\mathrm{s}(r) - V_\mathrm{ex}(r)$ and k, respectively, are the local kinetic energy and the relativistic wavenumber of the incident electron; $H(x)$ is Heaviside unit step function; Δ is the first excitation energy of the target atom; the m is the modification factor. It is well known that the effect of absorption potential should decrease with increasing energy. However, it is noted from Fig.1 that the difference between theoretical and experimental results increases with increasing energy for the absorption potential of Staszewska *et al* (expression (11)). This indicates that the effect of the absorption potential of Staszewska *et al* is increasing instead of decreasing with increasing energy. In addition, Raj and Tomar[22] and Staszewska *et al*[27] have observed that expression (11) overestimates the flux loss to the electronic excited states. In accordance with the above-stated analysis, the energy-dependent modification factor is empirically expressed as

$$m = \frac{1}{k - \sqrt{2\Delta}}, \tag{12}$$

where k and Δ, respectively, denote the relativistic wave number of the incident electron and the first excitation energy of the target atom. The value of modification factor m varies with different target atoms and decreases monotonically with the increase of incident energy of electrons. In numerical calculation, k and Δ are taken to be the values in atomic units. For every target atom, there is a critical energy E_c that corresponds to $m = 1$. Only if the incident energy of electron is greater than the critical energy of target atom, will the value of modification factor m be less than 1.0. The critical energy E_c is related to the target atom and can be calculated by the formula $E_\mathrm{c} = (1 + \sqrt{2\Delta/H})^2 H/2(\mathrm{eV})$, where the Hartree energy $H = 27.12\,\mathrm{eV}$ and Δ is in units of eV. Apparently the critical energy is an ascending function of Δ. When the incident energy of electron is less than the critical energy E_c, the value of m should be set to be 1.0 to assure the reasonable physical results. Table 1 shows the variations of the first excitation energy Δ, the critical energy E_c and the modification factor m with different target atoms and incident energy E of electrons. It is noted that the used value of the modification factor m is less than 1.0 and the incident energies of electrons are all greater than the critical energy of target atoms.

Table 1. The variations of the first excitation energy Δ, the critical energy E_c and the modification factor m with different target atoms and incident energy E of electrons.

atom	Δ	E_c	E/eV					
	/eV		100	150	200	300	500	700
H	10.20	47.37	0.5843	0.4309	0.3528	0.2705	0.1975	0.1619
C	1.26	23.15	0.5551	0.4148	0.3419	0.2641	0.1940	0.1596
F	12.70	52.60	0.6331	0.4568	0.3700	0.2805	0.2028	0.1655
S	1.15	22.67	0.5439	0.4085	0.3376	0.2615	0.1926	0.1587

3. Results and discussion

To compare the effects of modification of the absorption potential, Fig.1 displays the elastic differential cross sections for electron-CF_4 scattering at two incident energies. The solid curve represents the results obtained with the modified absorption potential (expression (10)), the short dash curve, with the unmodified absorption potential (expression (11)). It is evident from Fig.1 that, at the same incident energies, the DCS results of the solid curve and the short dash curve are almost the same for small scattering angles. However, for the rest of the scattering angles the two results differ from each other significantly. The results of the short dash curve are much lower than those of the solid curve. A comparison of our results with the experimental results of Sakae *et al*[38] shows that the results of the solid curve, obtained by using modified absorption potential, are in good agreement with the experimental data.

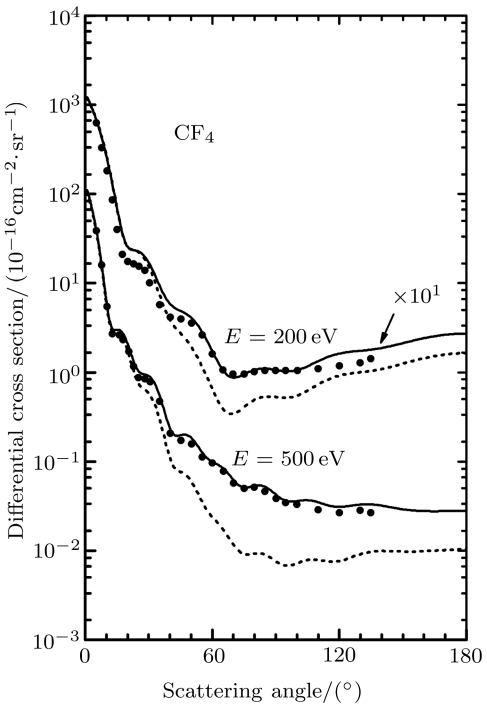


Fig.1. Elastic differential cross sections for electron-CF_4 scattering versus scattering angle at two incident energies separately by using the modified absorption potential (expression (10)) (solid curve); Staszewska *et al*'s absorption potential (expression (11)) (short dash curve); experimental data of Sakae *et al*[38] (full circle).

Figures 2 to 4 display the present results of the DCSs of electron-CH_4, electron-CF_4, and electron-SF_6 scatterings in the energy range of 100–700 eV, respectively. The solid curves represent the results obtained with using the full optical potentials and the dashed curves are for the results obtained without using the absorption potential. It is evident from these figures that the present results of DCS are generally in good agreement with the experimental data of Sakae *et al*[38] and give the same positions and depths of the DCSs dips as the experimental data. At higher incident energies the agreement is further improved and the present results turn closer to the experimental data. Although the qualitative natures of the solid and dashed curves are almost the same there can be a significant improvement on the value of DCS when the absorption effect is taken into account particularly in the middle and higher angular ranges of scattering angle. Furthermore the two curves merge into one another for low scattering angles ($\theta \leq 20°$).

It is noted from Figs.2 to 4 that, at large incident energies, the $\sin(qr_{ij})$ terms oscillate rapidly, resulting in more structures in molecular DCS at larger angles. As the number of atoms in the molecule increases and the molecule turns heavier and its structure becomes more complex, the DCSs of electron–molecule scattering show that there appear more structures at the same incident energy. This indicates that the structure of molecule manifests observable effects on electron–molecule scattering. In addition, it is noted that the DCSs of electron-CF_4 scattering display more complicated structures than those of electron-CH_4 scattering despite the fact that the two molecules are all composed of five atoms and belong to point group T_d. This means that the DCSs of electron–

molecule scattering are also related to the constituent of molecule.

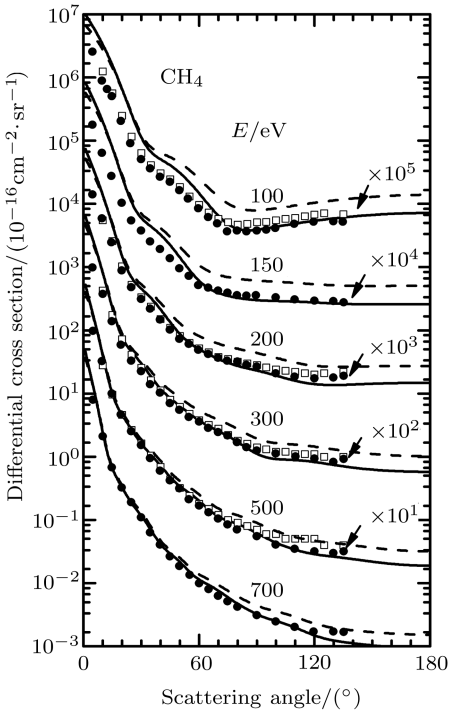


Fig.2. Elastic differential cross sections for electron-CH_4 scattering versus scattering angle at 100–700 eV obtained with using full potential (solid curve) and without using the absorption potential (dashed curve), and from experimental data of Iga *et al*[12] (open square); and Sakae *et al*[38] (full circle).

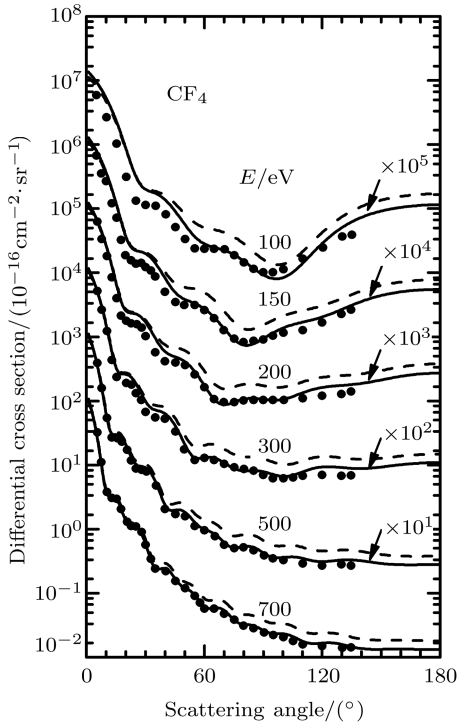


Fig.3. The same caption as that of Fig.2 except for electron-CF_4 scattering.

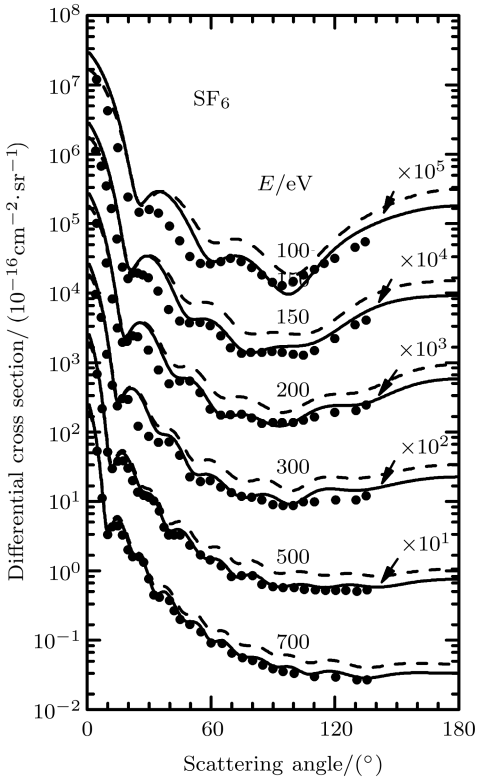


Fig.4. The same caption as that of Fig.2 except for electron-SF_6 scattering.

As the three figures show, the effect of absorption potential can cause the cross section to decrease, and it becomes small as the incident energy increases. Even if absorption potential is included, the present results overestimate DCSs as compared with the experimental data, especially at the low incident energies. This is because (i) the IAM neglects the multiple scattering and the valence bond distortion which are known to cause a reduction in the cross section,[39,40] especially for small scatterings and low incident energies; (ii) other structural effects (bonding environment, geometric shielding, etc) should reduce the atomic contributions compared with those in free atomic states.

4. Summary

By employing IAM together with the relativistic partial waves, we have calculated the DCSs for electron scattering from complex polyatomic molecules in an intermediate energy range. The application of the modified absorption potential in the present investigation has given the results in good agreement with the experimental data. This indicates that the present modification of the absorption potential of Staszewska

et al is successful and the IAM can provide reliable DCSs for electron scattering by molecule in this energy range. The present calculation also shows that the structure of the DCS of electron–molecule scattering is involved with the geometrical structure and constituent of the molecule. We may consider the IAM as a successful method to convert the molecular scattering problem into an atomic scattering problem which is easier to handle, in particular at higher incident energies. However, we have neglected the multiple scatterings and the valence bond distortion effects. For a complex polyatomic molecule the above effects may have appreciable effects on the cross sections. Hence further investigation including these effects should be performed. The present research is carried out for the highly symmetric molecules, so the application of the present method to the asymmetric/polar molecule is of interest.

References

[1] Trajmar S, Register D F and Chutjian A 1983 *Phys. Rep.* **97** 219
[2] Semenenko V A, Turner J E and Borak T B 2003 *Radiat. Environ. Biophys.* **42** 213
[3] Brunger M J and Buckman S J 2002 *Phys. Rep.* **357** 215
[4] Boudaiffa B, Cloutier P, Hunting D, Huels M A and Sanche L 2000 *Science* **287** 1658
[5] McCall B J and Oka T 2000 *Science* **287** 1941
[6] Gupta M and Baluja K L 2006 *Phys. Rev.* A **73** 042702
[7] Gianturco F A and Stoecklin T 1996 *J. Phys.* B **29** 3933
[8] Zheng Z, Chi B Q and Zhou Y J 2006 *Chin. Phys. Lett.* **23** 1169
[9] Tonzani S 2007 *Comput. Phys. Commun.* **176** 146
[10] Tonzani S and Greene C H 2006 *J. Chem. Phys.* **124** 054312
[11] Lane N F 1980 *Rev. Mod. Phys.* **52** 29
[12] Iga I, Lee M T, Homen M G P, Machado L E and Brescansin L M 2000 *Phys. Rev.* A **61** 022708
[13] Jain A and Baluja K L 1992 *Phys. Rev.* A **45** 202
[14] Sun J, Jiang Y and Wan L 1994 *Phys. Lett.* A **195** 81
[15] Jiang Y, Sun J F and Wan L D 1995 *Phys. Rev.* A **52** 398
[16] Sun J F, Bin X, Liu X F and Shi D H 2005 *Chin. Phys.* **14** 1125
[17] Shi D H, Liu Y F, Sun J F, Zhu Z L and Yang X D 2005 *Chin. Phys.* **14** 331
[18] Shi D H, Sun J F, Yang X D, Zhu Z L and Liu Y F 2005 *Acta Phys. Sin.* **54** 2019 (in Chinese)
[19] Liu Y F, Ma H, Shi D H, Sun J F and Zhu Z L 2006 *Acta Phys. Sin.* **55** 4096 (in Chinese)
[20] Liu Y F, Shi D H, Sun J F, Yang X D and Zhu Z L 2006 *Chin. Phys.* **15** 1278
[21] Walker D W 1968 *Phys. Rev. Lett.* **20** 827
[22] Raj D and Tomar S 1997 *J. Phys.* B **30** 1989
[23] McCarthy I E, Noble C J, Phillips B A and Turnbull A D 1977 *Phys. Rev.* A **15** 2173
[24] Green A E S, Rio D E and Ueda T 1981 *Phys. Rev.* A **24** 3010
[25] Thirumalai D and Truhlar D G 1982 *Phys. Rev.* A **26** 793
[26] Joachain C J, Vanderpoorten R, Winters K H and Byron Jr F W 1977 *J. Phys.* B **10** 227
[27] Staszewska G, Schwenke D W, Thirumalai D and Truhlar D G 1983 *Phys. Rev.* A **28** 2740
[28] Khare S P, Raj D and Sinha P 1994 *J. Phys.* B **10** 227
[29] Jain A 1986 *Phys. Rev.* A **34** 3707
[30] Jiang Y, Sun J and Wan L 1997 *Phys. Lett.* A **231** 231
[31] Jiang Y, Li J, Sun J and Wan L 2000 *Chin. J. At. Mol. Phys.* **17** 79
[32] Mott N F and Massey H S W 1965 *The Theory of Atomic Collisions* (Oxford: Oxford University Press)
[33] Walker D W 1971 *Adv. Phys.* **20** 257
[34] Salvat F 1987 *Phys. Rev.* A **36** 467
[35] Furness J B and McCarthy I E 1973 *J. Phys.* B **6** 2280
[36] Joachain C J 1975 *Quantum Collision Theory* (Amsterdam: North-Holland)
[37] Mittleman M H and Watson K M 1960 *Ann. Phys.* (N.Y.) **10** 268
[38] Sakae T, Sumiyoshi S, Murakami E, Matsumoto Y, Ishibashi K and Katase A 1989 *J. Phys.* B **22** 1385
[39] Hayashi S and Kuchitsu K 1976 *Chem. Phys. Lett.* **41** 575
[40] Jain A 1982 *J. Phys.* B **15** 1533